

Research Article

Terahertz Spectral Characteristics of Konjac Gum Determined via Microfluidic Technology

Huimin Jiang ¹, Qingjun Li ^{1,2,3,4}, Yan Shen ^{1,2,3,4}, Hangyu Zhou ¹, Yuchai Li ¹,
Bo Su ^{1,2,3,4} and Cunlin Zhang ^{1,2,3,4}

¹Department of Physics, Capital Normal University, Beijing 100048, China

²Key Laboratory of Terahertz Optoelectronics, Ministry of Education, Beijing 100048, China

³Beijing Key Laboratory for Terahertz Spectroscopy and Imaging, Beijing 100048, China

⁴Beijing Advanced Innovation Centre for Imaging Theory and Technology, Beijing 100048, China

Correspondence should be addressed to Bo Su; subo75@cnu.edu.cn

Received 29 March 2022; Revised 12 May 2022; Accepted 19 May 2022; Published 6 June 2022

Academic Editor: Haochong Huang

Copyright © 2022 Huimin Jiang et al. This is an open access article distributed under the Creative Commons Attribution License, which permits unrestricted use, distribution, and reproduction in any medium, provided the original work is properly cited.

Terahertz radiation enables nondestructive testing of biological samples, but is challenged by its high absorption in aqueous samples, so microfluidic technology is introduced to reduce the absorption. In this study, we designed a special temperature control device and an electric field device for a microfluidic chip to examine the terahertz spectral characteristics of konjac gum at different temperatures, concentrations, and electric field exposure time using the terahertz time domain spectroscopy system. Results demonstrate that higher concentrations of konjac gum lead to higher transmission intensity of terahertz radiation and a lower absorption of the radiation. Higher temperatures of the konjac gum lead to lower terahertz transmittance, and longer exposure time in the electric field leads to a lower transmittance of terahertz radiation and its higher absorption by the konjac gum. At the same time, we explain this phenomenon from the perspective of micromolecules. This study provides technical guidance for the detection of konjac gum by terahertz technology.

1. Introduction

Electromagnetic waves in the terahertz (THz) band have a frequency range of 0.1–10 THz and a wavelength range of 0.03–3 mm. They mark the transition zone from electronics to photonics. The research and applications of THz radiation are extensive, and the most prominent ones are in THz time domain spectroscopy (THz-TDS) technology [1, 2]. Several studies demonstrated that characteristic vibration modes of numerous biological macromolecules can be detected in the THz band [3–6]. These studies provide conditions for detecting biomolecules by THz technology. Ju et al. [7] used THz-TDS system to identify the presence of bt63 transgenic rice in nontransgenic rice in the range of 0.2–1.6 THz, principal component analysis was used to extract characteristic data, and the accuracy of sample identification reached 90%, providing a novel method for identifying transgenic components in rice. Cao et al. [8] analyzed the mixture of imidacloprid, carbendazim, and the flour matrix

using the THz-TDS system. Their results demonstrated that the THz-TDS system combined with Voigt function fitting and partial least squares can be used for the quantitative analysis of various pesticides in agricultural products with a small correction set. Bian et al. [9] measured the THz absorption spectra of L-lysine (Lys) and L-lysine hydrate (Lys H₂O) in the range of 0.3–2.5 THz using the THz-TDS system analyzed the vibration frequencies of Lys and Lys H₂O based on density functional theory and established the single molecule model of Lys and Lys H₂O. The results demonstrated that the collective vibration modes of Lys and Lys H₂O at different frequencies were derived from the dihedral torsion or bond angle bending of different molecular chains in a single molecule. These structural changes of Lys and Lys H₂O can be clearly observed by THz technology. The studies demonstrate the large role of THz technology in many fields.

Water plays a central role in the function of biomolecules; therefore, most experiments are performed in an aqueous solution. The interaction between hydrated

molecules in solution involves various biological phenomena, commonly known as hydration [10]. Hydrogen bonds between water molecules strongly interact with THz waves, and therefore, water exhibits strong absorption of THz radiation. Hence, it is difficult to examine biological samples by THz technology. Microfluidic technology is able to accurately manipulate fluids on the microscale. Therefore, the combination of THz technology and microfluidic technology can better identify fluid substances and detect their characteristics. Satti et al. [11] designed a centrifugal microfluidic chip to evaluate the chemotaxis of human neutrophils. Zhang et al. [12] made a microfluidic chip with thousands of channels made of silicon and probed the THz absorption signatures of the microcystin aptamer by using this chip and a coherent photomixing THz spectrometer. Experimental results showed that one remarkable signature around 830 GHz repeatedly appeared, which indicated that the THz spectrometer combined with a microfluidic chip can be used as an effective label-free technology to detect the THz spectral characteristics of biomolecules in solution. Baragwanath et al. [13] developed a microfluidic unit with Si as the substrate and tested the transmittance of the microfluidic unit by the THz-TDS system. The experimental result demonstrated that there were significant differences in the time domain spectra, refractive index, and other parameters of samples with different concentrations and types. Cai et al. [14] studied the effect of deionized water treated by an electric field for different time periods on THz absorption intensity by using a sandwich microfluidic chip. The results show that the transmission intensity of the THz wave increases with the time spend within deionized water in the electric field. Therefore, it is feasible to identify substances and examine their characteristics by the THz spectra based on a microfluidic chip.

Amorphophallus konjac is a food with low heat energy, low protein, and high dietary fiber and is rich in more than a dozen amino acids and trace elements required by the human body. As a functional food, konjac has a certain effect on hypertension, obesity, diabetes, and constipation. It is capable of draining toxins and garbage from the body and preventing colon cancer. It has multiple physical and chemical properties, such as water solubility, capability of thickening, stabilization, suspension, gel, film forming, and bonding, making it a natural health food and ideal food raw material. Konjac gum is primarily obtained from the tuber of plant konjac. Konjac glucomannan (KGM) is the unique primary component of konjac tuber. Figure 1 shows its molecular structure [15]. It is a high-molecular-weight heteropolysaccharide formed by D-glucose and D-mannose in the molar ratio of 1:1.6 and connected by β -1, 4 sugar sweet bond and β -1, 3 sugar sweet bond. The content of KGM in konjac gum is 44%–64%, and the remainder is starch and other polysaccharides. Acetyl groups forming every 9–19 sugar units along the KGM skeleton contribute to the dissolution of KGM [15]. The natural KGM exhibits two structures: one is α -type (amorphous) and the other is β -type (crystalline). Moreover, KGM, the main component of konjac gum, is a natural neutral polysaccharide, which can automatically absorb water and expand into gel solution

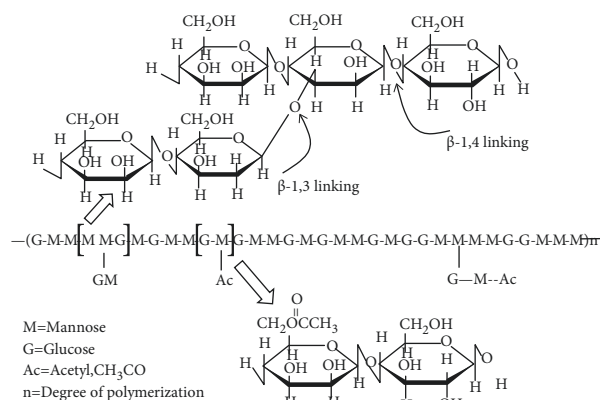


FIGURE 1: Molecular structure of KGM.

after being dissolved in it. It yields an elastic gel after alkali treatment, forming a thermally irreversible gel. Konjac flour dissolved in water can form konjac gum, a hydrophilic colloid. Konjac glucomannan can be used as a thickener, stabilizer, binder, and gel. It is extensively used in food, medicine, chemical industry, and other fields, and its development prospects are very extensive. Therefore, research on konjac gum holds extensive practical significance. However, there are few papers using THz technology to study colloids at present, so this study combined THz technology with microfluidic technology to study the THz spectrum of konjac gum. Because the konjac gum solution used in the experiments is a mixture of konjac flour and deionized water, THz-TDS and microfluidic technology may be combined to better examine the THz absorption characteristics of konjac gum. This provides a new method for the identification of colloids and a technical method for konjac gum to be better applied to food processing and chemical detection in the future. Compared with other technologies, THz waves can detect the characteristic vibration modes of many biological macromolecules, including konjac gum, and thus, THz waves can be used to obtain rich information about the structure and properties of substances. At the same time, the THz energy is of low intensity and facilitates nondestructive testing of the sample.

2. Experimental Device

2.1. Experimental Light Path. An in-house-constructed THz-TDS system was used in this work. The light source is a self-mode-locked fiber femtosecond laser purchased from Peking University, with a central wavelength of 1550 nm, pulse width of 75 fs, pulse repetition rate of 100 MHz, and power of 130 mW. The working principle of the whole system is as follows: the femtosecond laser is divided into two beams after passing through the polarized beam splitter (PBS). One beam is pump light, which is coupled into the optical fiber photoconductive antenna through the mechanical translation platform (bpca-100-05-101550-c-f of Batop company) to generate THz wave; the other beam is probe light, which is coupled to another photoconductive antenna (bpca-180-05-101550-c-f of Batop company) to detect THz wave. The fabricated microfluidic chip is placed

between two photoconductive antennas. The THz wave generated by the THz generation antenna carries the information of the sample after passing through the microfluidic chip filled with konjac gum solution, and then, the THz wave is received by the THz receiving antenna. Finally, the THz signal is amplified by the phase-locked amplifier, and then, the signal is collected and processed by the computer. A schematic of the experimental optical path is shown in Figure 2.

2.2. Fabrication of Microfluidic Chip. In this study, a new sandwich THz microfluidic chip is fabricated, which is mainly composed of three parts: substrate, cover, and microchannel layer. The material of substrate and cover is zeonor 1420R, which is an ideal material for preparing THz microfluidic chips. Its transmittance to THz waves can reach more than 85%, and there is no absorption peak. The size of the substrate and cover is $3\text{ cm} \times 2\text{ cm} \times 2\text{ mm}$. In addition, there were liquid inlet and outlet ports on the substrate and cover, respectively. The diameter of the liquid inlet and outlet is 2 mm. The middle is a $50\text{-}\mu\text{m}$ -thick strongly adhering double-sided adhesive, a hollow concave microchannel is carved in the middle of the double-sided adhesive, and the liquid outlet and liquid inlet are fixed at both ends of the concave microchannel. The depth of the microchannel is the thickness of konjac gum solution injected into the microfluidic chip. Figure 3 shows the process for preparing the microfluidic chip.

In order to test whether the fabricated microfluidic chip would be affected by temperature, the microfluidic chip without injection solution was heated in the range of $20\text{--}60$, and it was found that the THz wave transmittance had not changed, as shown in Figure 4. It can be seen that the microfluidic chip designed in this study was not affected by temperature, which provided a guarantee for the smooth progress of the experiment. Then, the microfluidic chip filled with konjac gum solution was heated. It was found that the microfluidic chip had no liquid leakage, indicating that the chip had a good sealing performance.

2.3. Temperature Control System. To control the temperature of the konjac gum, a high-precision temperature control system was designed. Its manufacturing method is to stick the microfluidic chip to a 2-mm-thick iron sheet with thermal conductive silica gel. A circular hole with a diameter of 8 mm is created on the iron sheet for THz waves to pass through. At the same time, the temperature sensor is secured to the same side of the iron sheet using thermal conductive silica gel. A circular alumina ceramic heating plate with holes (outer diameter is 40 mm and inner diameter is 10 mm) is bonded with thermal conductive silica gel on the other side of the iron sheet in order to heat the microfluidic chip. The heating plate and temperature sensor are controlled by the temperature controller (ST700 intelligent PID temperature controller). The rated voltage of the temperature controller is 220 V, the working frequency is 50–60 Hz, and the accuracy is 0.1°C . It can be adjusted in the range of $0\text{--}100^\circ\text{C}$. The temperature controller automatically controls the rise and

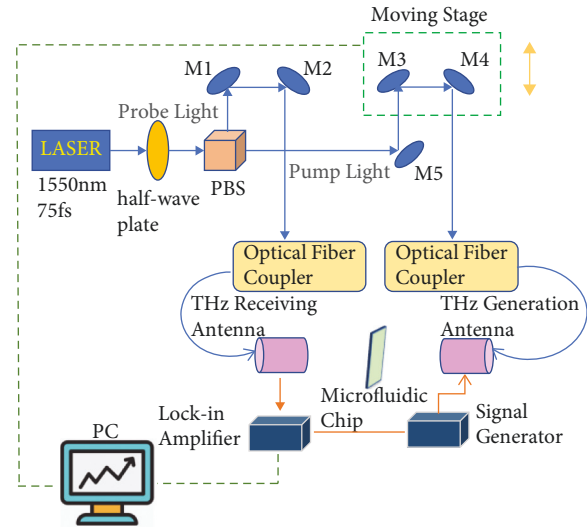


FIGURE 2: Diagram of the experimental light path.

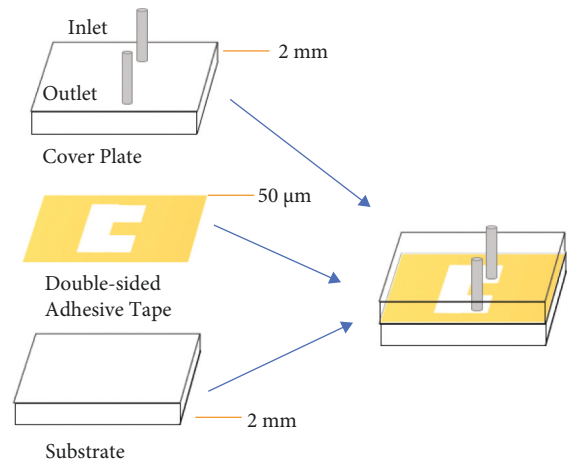


FIGURE 3: Fabrication process of the microfluidic chip.

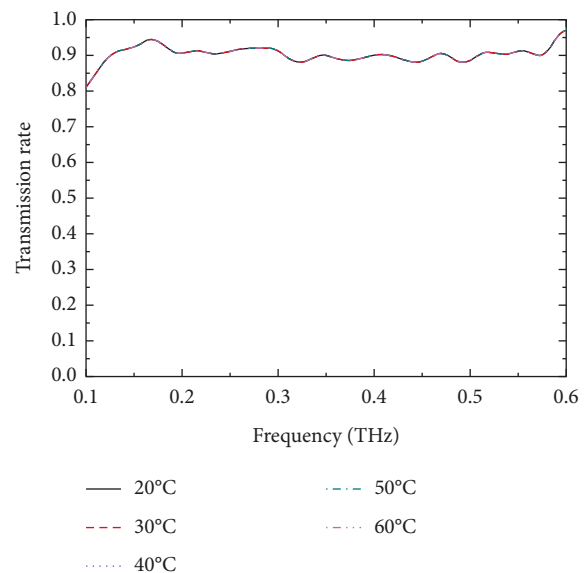


FIGURE 4: THz transmittance of substrate at different temperatures.

fall of the temperature, and the temperature controller can dynamically correct the temperature to maintain a constant value close to the target temperature. Figure 5 shows the temperature control device. In the experiment, the temperature sensor is pasted on the patch, so the detected temperature cannot be completely consistent with the temperature of konjac gum solution in the microfluidic chip. Therefore, this paper indirectly and qualitatively reflects the temperature change characteristics of the sample through the gradient temperature rise.

2.4. External Electric Field Device. A schematic diagram of the external electric field device utilized in the experiment is shown in Figure 6. A high-voltage power supply (dw-p153-05c51) is used to provide power. The two electrodes of the high-voltage power supply are connected with two metal plates, respectively, and a uniform electric field is generated by two parallel metal plates. In order to ensure the uniformity of the electric field through the microfluidic chip, the size of the two metal plates is much larger than that of the microfluidic chip. Then, the microfluidic chip that has been injected with konjac gum solution is placed vertically between the two metal plates and the power switch is turned on. After standing in the electric field for different time periods, the transmission characteristics of microfluidic chip are tested by THz-TDS system.

3. Experiment

3.1. THz Spectral Characteristics of Konjac Gum Solution at Different Temperatures. Konjac gum solution was prepared by adding 0.05 g konjac flour (Hubei Konson Konjac Gum Co., Ltd) to 50 mL of deionized water at room temperature (25°C), and then, the mixture was evenly stirred and heated in a water bath, resulting in 0.1% konjac gum solution [16]. The optimum water bath temperature for konjac gum solution is 50.0–60.0°C. After preparation, konjac gum was left to rest for 8 hours to yield a more uniform solution and better swelling conditions. By irradiating the solution with a laser pointer, a distinct Tindal effect can be observed, indicating that the solution is a colloid. The prepared konjac gum solution was injected in the microfluidic chip and probed by the THz-TDS system with 10°C increments. The temperature control system used to heat the microfluidic chip is shown in Figure 4, and the temperature variation range was set from 30 to 60°C. When the temperature reaches 65°C, the konjac gum solution in the chip produces bubbles because of an extremely high temperature, and when it is heated to 80°C, it almost becomes an aqueous solution and loses its viscosity. Both of these scenarios have an effect on the experimental results. To ensure the accuracy of the experimental results, each temperature gradient was repeated three times and all subsequent experiments in this study were treated in the same way. The THz frequency domain spectra of konjac gum solution at different temperatures are shown in Figure 7. Higher temperatures of the konjac gum solution lead to lower transmission intensities of THz and higher absorption of konjac gum to THz radiation.

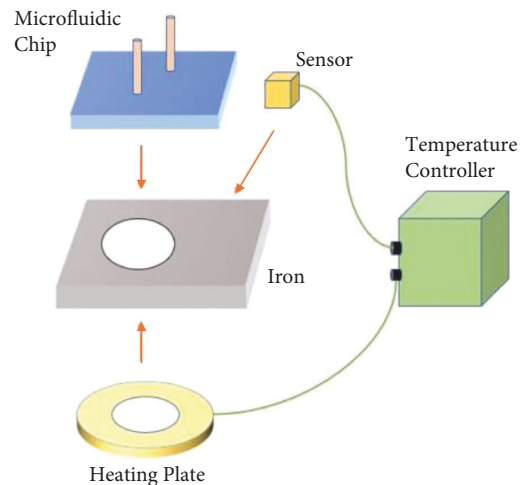


FIGURE 5: Schematic diagram of the temperature control system.

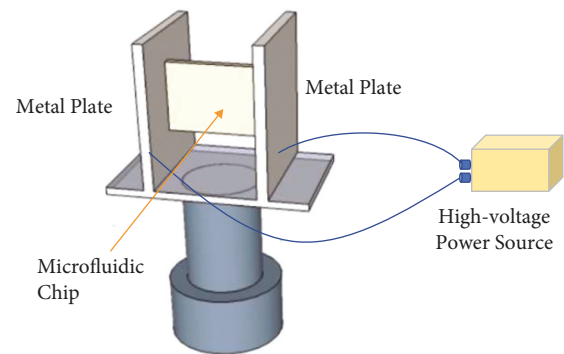


FIGURE 6: Schematic diagram of the electric field device.

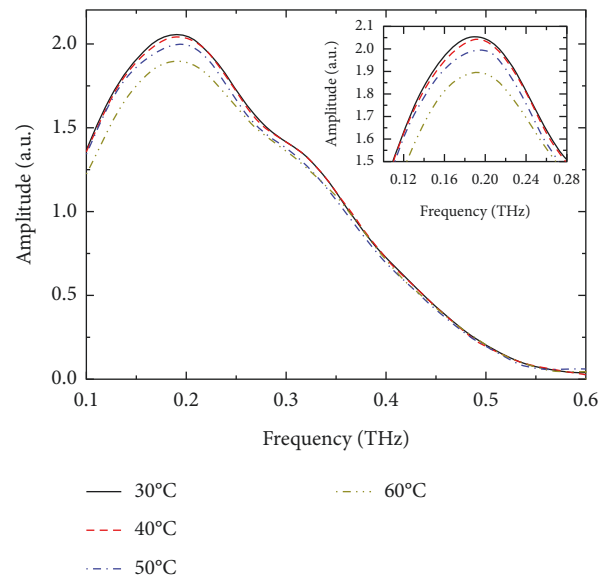


FIGURE 7: Spectra of konjac gum solution at different temperatures.

3.2. THz Spectral Characteristics of Konjac Gum Solution at Different Concentrations. Three konjac gum solutions with concentrations of 0.1%, 0.2%, and 0.3% were prepared with

deionized water and subsequently injected in the microfluidic chip. The chip was placed into the THz-TDS system and tested to obtain the spectra diagram shown in Figure 8. THz holds the greatest transmission intensity via deionized water. Higher concentrations of konjac gum solution lead to higher transmission intensities of THz and lower absorption of konjac gum to THz radiation.

3.3. THz Spectral Characteristics of Konjac Gum Solution in External Electric Field. The konjac gum solution with a concentration of 0.1% was injected in the microfluidic chip, and its THz spectrum was obtained without an electric field via the THz-TDS system. Then, the microfluidic chip injected with konjac gum solution was vertically placed between two metal plates, and an electric field was applied to it using the external electric field device with an electric field strength of 2500 V/cm. The effect of electric field on konjac gum was examined by varying the standing time of the microfluidic chip in the electric field. In this experiment, three time gradients are set with a measurement interval of 10 min and a measurement range of 0–20 min. The THz spectra are shown in Figure 9. The peak value of THz changes with the standing time in the electric field. A longer standing time leads to a lower THz transmission intensity and stronger THz absorption.

4. Discussion

The THz spectra of the konjac gum solutions at different temperatures show that the transmission intensity of THz decreases with the increase in temperature. This is in contrast to the theoretical analysis, which indicates that a temperature increase will lead to hydrogen bond breaks and therefore enhanced THz transmission intensity. Preliminarily, we consider that KGM, the primary component of konjac gum, is a large polymer having a high molecular weight. With an increase in the temperature, the molecular thermal movement intensifies, and the aggregate size decreases. Certain KGM molecules break away from KGM macromolecular clusters because of hydrogen bond fracture [16], forming small konjac gum molecular clusters. The vibration and rotation of molecules separated from hydrogen bonds are strengthened because of their thermal movement. During this process, the absorption of the THz wave caused by the increase of small konjac gum molecular clusters and the intensification of thermal movement is stronger than the absorption of the THz wave reduced by molecules breaking away from the hydrogen bonds. Therefore, with the increase in temperature, the THz transmission intensity decreases, and the absorption of THz by konjac gum increases.

The THz spectra of konjac gum solutions at different concentrations show that the transmission intensity of THz increases with increase in konjac gum concentration in solution. The results show that an increase in the konjac gum concentration leads to the intertwining of KGM polymers and increase in the resistance of the fluid and the viscosity. However, when the concentration of konjac gum solution is

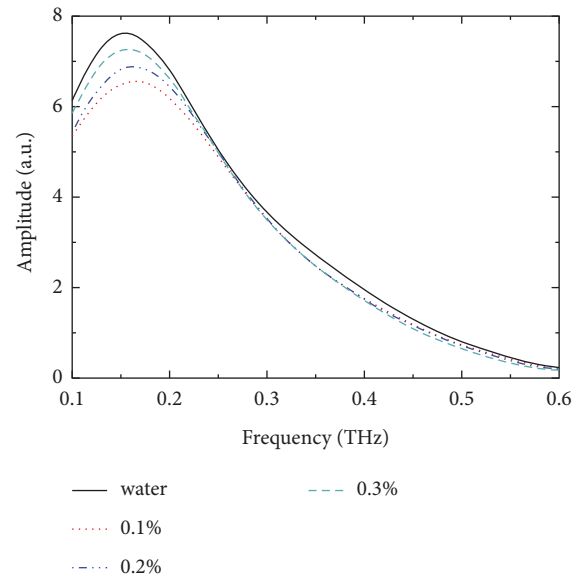


FIGURE 8: Spectra of konjac gum solution at different concentrations.

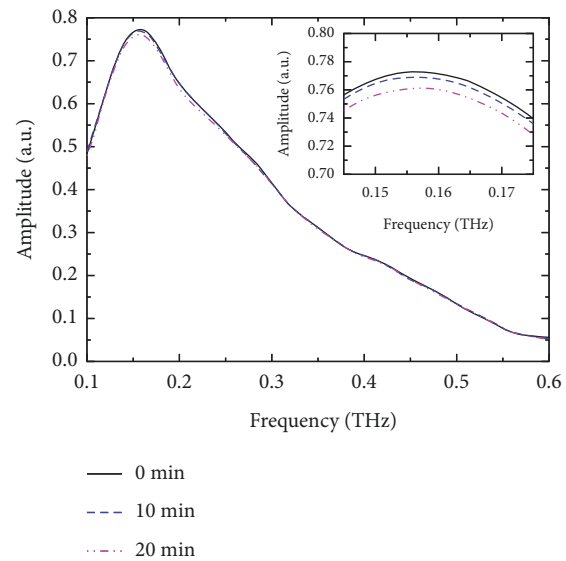


FIGURE 9: Spectra of konjac gum spent in electric field for different periods of time.

low (<0.4%), the increase in the viscosity is relatively small [16]. With the increase in viscosity, the forces between molecular chains increase, the number of hydrogen bonds increases, and consequently, the THz absorption of konjac gum rises [10]. In this study, the highest concentration of konjac gum solution is 0.3% such that the increase in the number of hydrogen bonds because of the increase in viscosity is miniscule. Joanna et al. [17] reported that the increase in konjac gum concentration will reduce the elasticity of the biopolymer chain. Furthermore, with increase in konjac gum concentration, the number of polymer molecular chains compared to the solvent rises, the molecular chains break because of insufficient elasticity during extension, and the number of hydrogen bonds decreases. The

reduction in the number of hydrogen bonds because of molecular chain breaking is more than the increase in the number of hydrogen bonds caused by the increase in abovementioned viscosity. Therefore, the THz absorption of konjac gum decreases. Liu et al. [18] studied the refractive index (n) and absorption coefficient (α) of blue phase liquid crystal samples using formulas (1) and (2), respectively.

$$n = 1 + \frac{c}{\omega d} (\phi_{\text{sample}} - \phi_{\text{COC}}), \quad (1)$$

$$\alpha = -\frac{2}{d} \ln \frac{[n + 1]^2 \left| \frac{E_{\text{sample}}}{E_{\text{COC}}} \right|}{4n}, \quad (2)$$

where c is the speed of light in vacuum, ω is the angular frequency of the THz wave, and d is the thickness of the sample. If the refractive index of air is set to 1, ϕ_{sample} , ϕ_{COC} , E_{sample} , and E_{COC} are the phase and amplitude of the THz field passing through the sample and the COC empty chip, respectively. The THz absorption coefficient of konjac gum with different concentrations was calculated by using formulas (1) and (2), as shown in Figure 10. The THz absorption coefficient of water in this study is similar to the results of Thrane et al. [19] and Son et al. [20]. It can be seen that the absorption coefficient decreases with the increase of concentration, which is consistent with the trend observed in the experiment; that is, the increase of konjac gum concentration corresponds to the increase of transmission intensity.

The THz spectra of konjac gum standing in the electric field for different time periods show that longer standing time lead to lower transmission intensities of THz and higher THz absorption of konjac gum. This is in contrast to the result claiming that longer standing time of deionized water in the electric field leads to higher transmission intensity of THz spectra [14], indicating that application of the electric field has a certain effect on the konjac gum solution. The study demonstrates that in the absence of an external electric field, the orientation of molecules in the solution is disordered, and the optical anisotropy effect of each molecule is canceled out. Under the action of an applied electric field, the molecules are arranged along the direction of the electric field, which increases the rigidity of the molecular chain [10], as shown in Figure 11. With the increase in the exposure time of the konjac gum solution in the electric field, the effect of electric field force may disengage the acetyl group on the side chain of KGM molecule, enhancing the agglomeration ability of KGM molecules [21] and increasing the hydrogen bonding between molecules. Therefore, the THz absorption of konjac gum rises. Similarly, the THz absorption coefficient of konjac gum under different electric field exposure time periods was calculated using the above method, as shown in Figure 12. It can be seen that the absorption coefficient increases in direct proportion to the time spent within the electric field, which further shows that the experimental results are correct.

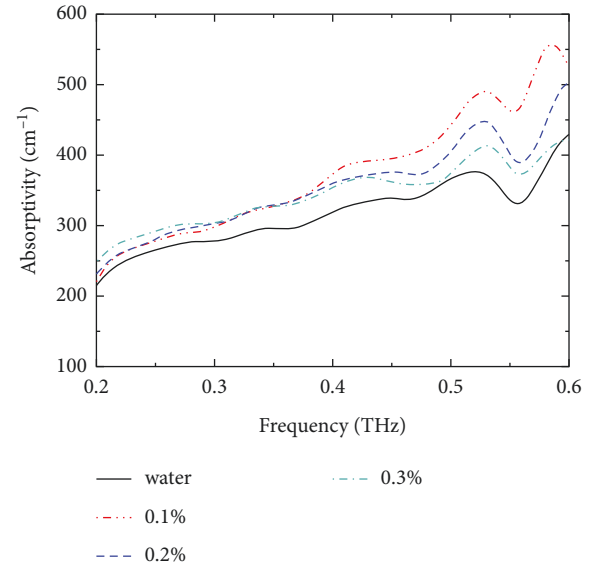


FIGURE 10: THz absorption coefficient of konjac gum at different concentrations.

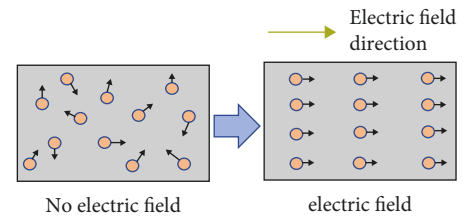


FIGURE 11: Molecular changes in konjac gum solution after applying an electric field.

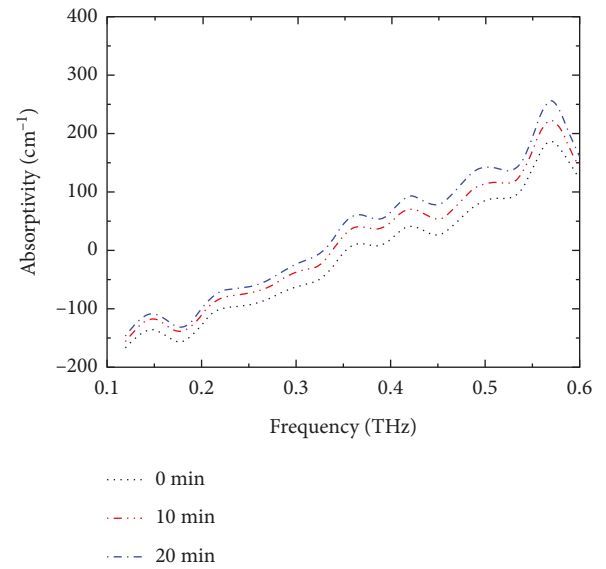


FIGURE 12: THz absorption coefficient of konjac gum under different electric field exposure time periods.

5. Conclusion

This study introduces a novel fabrication method for a THz microfluidic chip. This chip has the advantages of a short manufacturing time, no liquid leakage, and temperature dependence. In addition, the material used for the substrate and cover plate of the microfluidic chip is zeonor 1420R with high transmittance to THz waves. Furthermore, to examine the effects of different temperatures on the konjac gum solution, we designed a high-precision temperature control system. Experimental results demonstrate that the THz transmission intensity decreases with the increase in temperature. The THz spectra of different concentrations of konjac gum solutions demonstrated that the transmission intensity of THz increases with increasing concentration. Finally, we studied the THz spectral characteristics of konjac gum solution with different standing time periods in a strong electric field. Compared with no electric field, the THz transmission intensity decreases with increase in the standing time. The combination of the microfluidic chip and THz-TDS provides technical guidance for the detection of konjac gum, provides a new method for identifying colloids, and lays a foundation to expand research related to THz technology.

Data Availability

The data used to support the findings of this study are available from the corresponding author upon request.

Conflicts of Interest

The authors declared that they have no conflicts of interest.

Authors' Contributions

All authors contributed to the theoretical analysis, calculations, experiment, and preparation of the manuscript.

Acknowledgments

This work was supported by the National Natural Science Foundation of China (NSFC) (61575131). The authors would like to thank "Enago" for providing English touch-up.

References

- [1] J. Q. Yang, S. X. Li, H. W. Zhao et al., "Terahertz study of L-asparagine and its monohydrate," *Acta Physica Sinica*, vol. 63, no. 13, pp. 105–111, 2014.
- [2] J. Neu, H. Nikonow, and C. A. Schmuttenmaer, "Terahertz spectroscopy and density functional theory calculations of DL-norleucine and DL-methionine," *The Journal of Physical Chemistry A*, vol. 122, no. 28, pp. 5978–5982, 2018.
- [3] Y. Kawano, "Terahertz waves: a tool for condensed matter, the life sciences and astronomy," *Contemporary Physics*, vol. 54, no. 3, pp. 143–165, 2013.
- [4] D. B. Bennett, Z. D. Taylor, P. Tewari et al., "Assessment of corneal hydration sensing in the terahertz band: in vivo results at 100 GHz," *Journal of Biomedical Optics*, vol. 17, no. 9, Article ID 0970081, 2012.
- [5] K. Shiraga, Y. Ogawa, N. Kondo, A. Irisawa, and M. Imamura, "Evaluation of the hydration state of saccharides using terahertz time-domain attenuated total reflection spectroscopy," *Food Chemistry*, vol. 140, no. 1–2, pp. 315–320, 2013.
- [6] D. B. Hou, X. Li, J. H. Cai et al., "Terahertz spectroscopic investigation of human gastric normal and tumor tissues," *Physics in Medicine and Biology*, vol. 59, no. 18, pp. 5423–5440, 2014.
- [7] X. G. Ju, Y. Zhang, F. Y. Lian, and Mx Fu, "Quick test for transgenic components in rice using terahertz spectra," *Applied Spectroscopy*, vol. 73, no. 2, pp. 171–181, 2019.
- [8] B. H. Cao, H. Li, E. Cai, and M. Fan, "Determination of pesticides in flour by terahertz time-domain spectroscopy (THz-TDS) with Voigt function fitting and partial least squares (PLS) analysis," *Analytical Letters*, vol. 54, no. 5, pp. 830–841, 2021.
- [9] Y. J. Bian, X. Zhang, Z. Q. Zhu, and Y. Bin, "Vibrational modes optimization and terahertz time-domain spectroscopy of L-Lysine and L-Lysine hydrate," *Journal of Molecular Structure*, vol. 1232, 2021.
- [10] F. X. Zhang, G. Y. Wang, H. Y. Huang et al., "Terahertz absorption characteristics of guar gum determined via microfluidic technology," *Journal of the European Optical Society-Rapid Publications*, vol. 17, no. 1, 2021.
- [11] S. Satti, P. Deng, K. Matthews, S. P. Duffy, and H. Ma, "Multiplexed end-point microfluidic chemotaxis assay using centrifugal alignment," *Lab on a Chip*, vol. 20, no. 17, pp. 3096–3103, 2020.
- [12] M. K. Zhang, Z. B. Yang, M. J. Tang et al., "Terahertz spectroscopic signatures of microcystin aptamer solution probed with a microfluidic chip," *Sensors*, vol. 19, no. 3, p. 534, 2019.
- [13] A. J. Baragwanath, G. P. Swift, D. Dai, A. J. Gallant, and J. M. Chamberlain, "Silicon based microfluidic cell for terahertz frequencies," *Journal of Applied Physics*, vol. 108, no. 1, Article ID 13102, 2010.
- [14] Y. Cai, J. H. Wang, Z. C. Bai, S. U. Bo, and C. L. Zhang, "Terahertz transmission characteristics of water induced by electric field," *Spectroscopy and Spectral Analysis*, vol. 41, no. 6, pp. 1683–1687, 2021.
- [15] K. Nishinari, P. A. Williams, and G. O. Phillips, "Review of the physico-chemical characteristics and properties of konjac mannan," *Food Hydrocolloids*, vol. 6, no. 2, pp. 199–222, 1992.
- [16] Y. L. Wang, Z. H. Li, and Y. Wei, "Rheology and influence factor of low-concentration Konjac gum solutions," *Journal of Central South University of Technology*, vol. 15, pp. 516–519, 2008.
- [17] K. Joanna, K. Kaczmarczyk, A. Ptaszek, U. Goik, and P. Ptaszek, "The effect of temperature on the colligative properties of food-grade konjac gum in water solutions," *Carbohydrate Polymers*, vol. 174, pp. 456–463, 2017.
- [18] Q. F. Liu, D. Luo, X. H. Zhang, S. Li, and Z. Tian, "Refractive index and absorption coefficient of blue phase liquid crystal in terahertz band," *Liquid Crystals*, vol. 44, 2017.
- [19] L. Thrane, R. Jacobsen, P. Uhd Jepsen, and S. Keiding, "THz reflection spectroscopy of liquid water," *Chemical Physics Letters*, vol. 240, no. 4, pp. 330–333, 1995.
- [20] H. Son, D. H. Choi, and G. S. Park, "Improved thickness estimation of liquid water using kramers–kronig relations for determination of precise optical parameters in terahertz transmission spectroscopy," *Optics Express*, vol. 25, no. 4, p. 4509, 2017.
- [21] C. Zhang, F. Q. Yang, and J. D. Chen, "Konjac glucomannan, a promising polysaccharide for OCDDS," *Carbohydrate Polymers*, vol. 104, no. 1, pp. 175–181, 2014.